CWE-8
June 7-11, 2026
London, ON, Canada

Evaluation of synthetic turbulence generation for LES-based wind load estimation on square buildings

Long Doan Sy [a], Chisato Kojima [b], Manabu Kawashima [c], Yuichi Hirata [d], Hiroshi Noda [e]

[a]*Sumitomo Mitsui Construction Co., Ltd., Nagareyama, Chiba, Japan, doansylong@smcon.co.jp*
[b]*Sumitomo Mitsui Construction Co., Ltd., Nagareyama, Chiba, Japan, c-kojima@smcon.co.jp*
[c]*Sumitomo Mitsui Construction Co., Ltd., Nagareyama, Chiba, Japan, mkawashima@smcon.co.jp*
[d]*Sumitomo Mitsui Construction Co., Ltd., Nagareyama, Chiba, Japan, YuichiHirata@smcon.co.jp*
[e] *Kindai University, Higashi-Osaka, Osaka, Japan, hnoda@arch.kindai.ac.jp*

SUMMARY

This study evaluates the Consistent Discrete Random Flow Generation (CDRFG) method for Large Eddy Simulation (LES)-based wind load estimation on square-cylinder buildings. Wind tunnel experiments and CFD simulations confirm that CDRFG reproduces target turbulence statistics and yields reasonable agreement for total wind force coefficients in the principal directions. Non-physical pressure fluctuations are nevertheless observed, attributed to limits in enforcing the divergence-free condition in the synthetic inflow. The study clarifies the origin of these artifacts and proposes mitigation strategies, providing a pathway to reduce residual effects and enhance the applicability of CDRFG in LES-based wind load assessment.

Keywords: *LES, synthetic turbulence generator, random flow generation, CDRFG, wind tunnel, square cylinder*

1. INTRODUCTION

Synthetic turbulence generation methods are favored for their flexibility in controlling turbulence statistics. Synthetic turbulence generation has evolved significantly since the foundational Random Flow Generation (RFG) method by Kraichnan (1970). The Consistent Discrete Random Flow Generation (CDRFG) method of Aboshosha et al. (2015), incorporating frequency-dependent spatial scaling and tuning factors, produces turbulent inflow conditions that closely match target wind statistics and coherency. Moreover, when applied as an LES inflow, CDRFG yields wind force predictions on building models that agree well with wind tunnel results.

According to Zhang et al. (2022), the RMS value of the pressure coefficients on the building model surfaces is significantly higher when the CDRFG method is applied at the inlet boundary. However, the authors do not provide a detailed explanation for this result. In the present study, the reported artificial pressure fluctuations are confirmed through comparison with wind tunnel test results. These fluctuations arise due to the synthetic inflow failing to fully comply with the divergence-free constraint. The underlying causes are explained using mathematical analysis, and possible directions for improving the inflow generation method are discussed.

2. METHODOLOGY

The wind tunnel (WT) experiments are conducted at Sumitomo Mitsui Construction Company, assuming the ground surface roughness Category III as defined by Architectural Institute of Japan (AIJ). A gradient flow with a power-law exponent of $\alpha = 0.2$ is simulated, and the reference wind

speed $U_{\mathrm{H}} = 10m/s$ at the reference height $H = 0.3m$. The WT experiments are performed for wind approach angles ranging from 0° to 355°, in 5° increments, with 10 samples (each representing a 10-minute dataset) collected for each angle. For the present analysis, only the data corresponding to the 0° wind direction are utilized. The pressure-tapped model has dimensions $B \times D \times H = 0.1\mathrm{m} \times 0.1\mathrm{m} \times 0.3\mathrm{m}$ at geometric scale of $1:400$ to prototype building.

OpenFOAMv2106 with Smagorinsky model $Cs = 0.14$ is employed in LES analysis. The domain spans $90B$ (streamwise, u), $21B$ (crosswind, v), and $18B$ (vertical, w), with the inlet at $x = -10.5B$ and the model at $x = 0$. An unstructured tetrahedral mesh, divided into seven zones, follows the AIJ guidelines (Architectural Institute of Japan, 2017). Two adjustments are introduced: the refined mesh region around the model is extended upstream to the inlet to better resolve incoming turbulence, and the downstream domain is lengthened to ensure sufficient flow development. These modifications result in approximately 36.8 million computational cells in total. At the inlet, the CDRFG algorithm is derived based on the WT wind profile results, and synthetic turbulent velocity fields in the u, v, and w components are generated at each inlet mesh face center.

3. RESULTS

Figure 1 presents the streamwise flow properties for CDRFG inflow generation (labeled "Inflow") and for an empty-domain simulation (same inflow algorithm on a domain without the building model). The CDRFG method reproduces mean wind speed and turbulence intensity (Figure 1a., b.) that are close to the target WT results, while the power spectral density (PSD) (Figure 1e.) follows the Von Karman spectrum. In addition, the wind characteristics are generally well preserved along the streamwise direction: The mean wind speed remains nearly constant, whereas the turbulence intensity shows a slight downstream decay. The "Near inlet" label in Figure 1 denotes the first mesh location immediately downstream of the inlet, and the profiles at $x = -10B, -5B\ and\ 0$ correspond to empty-domain results extracted along the centerline ($y = 0$). The decrease in turbulence intensity is primarily caused by attenuation of high-frequency energy, as evidenced by the PSD in Figure 1e. Nevertheless, the low-frequency range relevant to wind-induced building response ($nB/U = 0.2{\sim}0.4$) continues to follow the Von Karman spectrum.

Figure 1c. and d. present the pressure coefficient statistics in the empty-domain simulation. The mean pressure coefficient ($\overline{C_p}$) remains close to zero throughout the domain, whereas the standard deviation (σ_{C_p}) shows relatively large values. At the model location, the pressure fluctuation reaches $\sigma_{C_p} = 1.07$, indicating a pronounced non-physical pressure fluctuation in the domain.

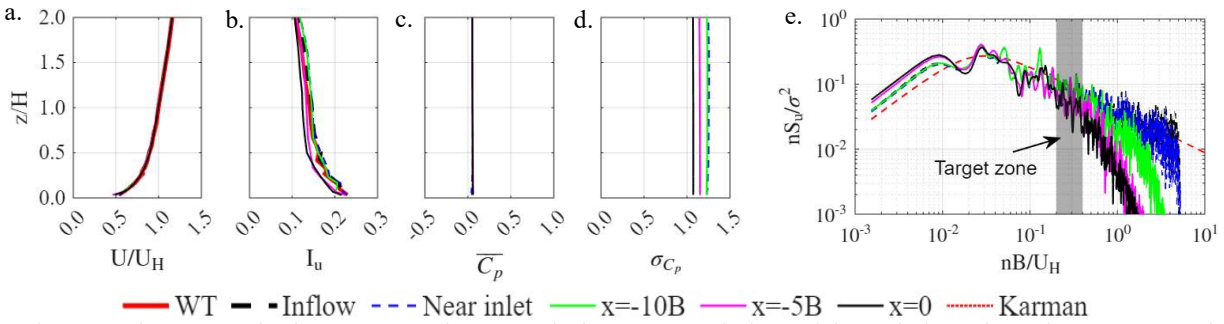

Figure 1: Flow properties in CDRFG and ABL analysis: a. Mean wind speed, b. Turbulence intensity, c. Mean and d. Standard deviation of pressure coefficients, and e. Power spectrum at model height

Table 1 compares the total wind force coefficients (pressure integrated over all faces) and the face-specific contributions (integration over each face) obtained from the WT experiments and CFD simulations. The CFD predictions of mean total coefficients ($\bar{C_F}$) show good agreement with the WT results. For the standard deviations (σ_{C_F}), the CFD values, computed from a single simulation, are generally larger for the force components ($\sigma_{C_{Fx}}$, $\sigma_{C_{Fy}}$, and $\sigma_{C_{Fz}}$) than the WT values, which represent the average of ten samples. This trend is consistent with Zhang et al. (2022). Similar overestimations appear in most moment components except for the rotational moment C_{Mz}. In general, components associated with opposing faces (C_{F_x}, C_{F_y}, C_{M_x}, and C_{M_y}), and the counteracting moment (C_{Mz}) are well reproduced for total wind force coefficients, whereas components without counterparts, such as C_{Fz}, show markedly larger σ_{C_F} in CFD than in WT.

The PSD of total wind force and overturning moment coefficients in Figure 2 further confirms good agreement between CFD and WT in the along-wind and across-wind directions. The red dashed line ("AIJ Eq.") shows spectra from AIJ guidelines, and WT results are plotted as envelopes, "WT min" and "WT max," corresponding to the minimum and maximum spectra from the WT ensemble. The CFD spectra fall within this WT range. In contrast, the vertical force, lacking an opposing surface, exhibits substantially larger standard deviations in CFD, consistent with the elevated vertical in Table 1.

Table 1: Comparison of wind force coefficients on building model (mean value $\bar{C_F}$ ± standard deviation value σ_{C_F})

		Front	Right	Rear	Left	Roof	Total
C_{F_x}	WT	0.593±0.181	--	0.366±0.113	--	--	0.958±0.269
	CFD	0.585±1.024	--	0.429±1.024	--	--	1.014±0.266
C_{F_y}	WT	--	-0.667±0.218	--	0.662±0.211	--	-0.005±0.301
	CFD	--	-0.635±1.031	--	0.633±1.055	--	-0.002±0.379
C_{F_z}	WT	--	--	--	--	0.752±0.181	0.752±0.181
	CFD	--	--	--	--	0.702±1.022	0.702±1.022
C_{M_x}	WT	--	0.346±0.110	--	-0.344±0.107	-0.006±0.004	-0.004±0.153
	CFD	--	0.325±0.514	--	-0.321±0.525	-0.001±0.002	0.003±0.179
C_{M_y}	WT	0.324±0.100	--	0.191±0.060	--	0.006±0.004	0.522±0.145
	CFD	0.317±0.509	--	0.226±0.512	--	0.001±0.002	0.544±0.138
C_{M_z}	WT	0.000±0.018	0.027±0.033	0.000±0.016	-0.027±0.033	--	0.000±0.061
	CFD	-0.001±0.014	0.005±0.023	0.000±0.022	-0.001±0.017	--	0.003±0.040

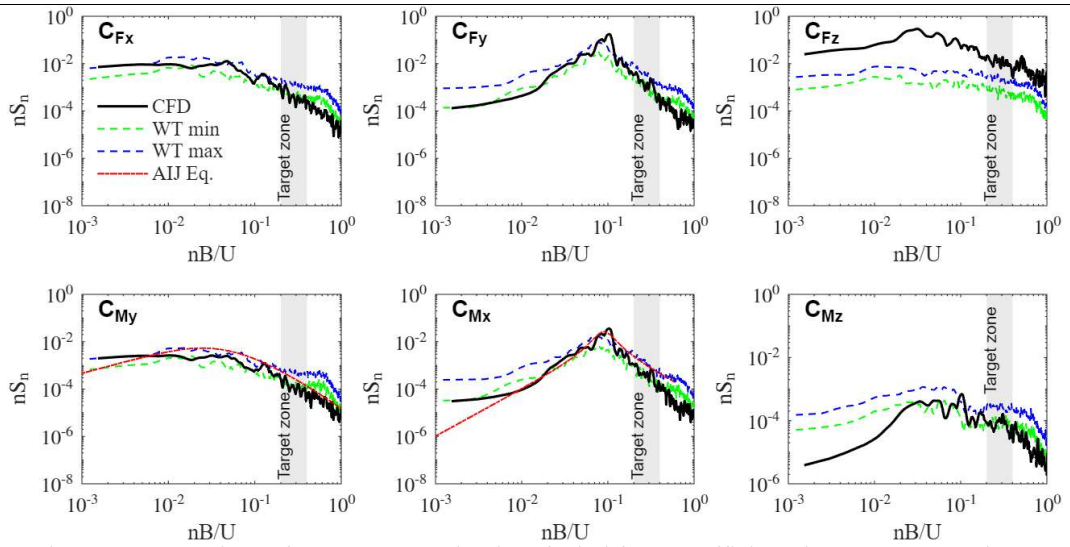

Figure 2: Comparison of power spectra density of wind force coefficients between CFD and WT

4. DISCUSSION AND CONCLUDING REMARKS

This study applies LES with the CDRFG method for synthetic turbulence at the inlet, demonstrating that wind force and overturning moment components on opposing building faces show strong agreement with wind tunnel experiments. Non-physical pressure fluctuations arise from imperfect enforcement of the divergence-free condition in the synthetic inflow, but these effects are largely canceled in total force components due to the net contribution from paired surfaces with opposite pressures. As a result, both mean values and standard deviations of total force coefficients match well between CFD and experimental results.

Ideally, in the absence of obstacles, the pressure field should exhibit negligible fluctuations if the divergence-free condition prescribed by the continuity equation is fully satisfied. However, the observed pressure statistics in Figure 1d. indicate a substantial deviation from this condition. Although the CDRFG method has generally been considered divergence-free, the present results indicate that this assumption does not hold. In the Eq. (1) for synthetic velocity field $u_i(x_j, t)$

$$u_i(x_j, t) = \sum_{m=1}^{M} \sum_{n=1}^{N} p_i^{m,n} cos\left(k_j^{m,n} \frac{x_j}{L_j^m} + 2\pi f_{n,m} t\right) + q_i^{m,n} sin\left(k_j^{m,n} \frac{x_j}{L_j^m} + 2\pi f_{n,m} t\right) \quad (1)$$

in CDRFG method (parameters and suffixes are referred to Aboshosha et al. (2015)), the nondimensional spatial coordinate x_j/L_j^m is used. Taking the divergence of synthetic velocity field $\nabla u_i(x_j, t)$ yields terms proportional to $p_i^{m,n} k_j^{m,n}/L_j^m$ and $q_i^{m,n} k_j^{m,n}/L_j^m$. Therefore, to satisfy the divergence-free condition $\nabla u_i(x_j, t) = 0$, the two coefficients must be mutually orthogonal so that their contributions form a solenoidal (divergence-free) vector field. Consequently, the velocity field is inferred to contain residual divergence, which is considered likely to contribute to the non-physical pressure fluctuations observed in the empty-domain simulation.

Potential approaches to mitigate these non-physical fluctuations include: (i) improving the implementation of the CDRFG method to enforce proper divergence with respect to L_j^m; and (ii) applying numerical correction using Poisson equation to remove pressure gradient components from the synthetic velocity fields as also applied in Zhang et al. (2022). These approaches represent promising directions, but their practical realization remains a subject for future work.

ACKNOWLEDGEMENTS

The authors wish to thank the Information Technology Center at the University of Tokyo for providing access to the High-Performance Computing system through the corporate use program.

REFERENCES

Aboshosha, H., Elshaer, A., Bitsuamlak, G.T., El Damatty, A., 2015. Consistent inflow turbulence generator for LES evaluation of wind-induced responses for tall buildings. Journal of Wind Engineering and Industrial Aerodynamics 142, 198-216.

Architectural Institute of Japan, 2017. Guidebook of Recommendations for Loads on Buildings, Vol. 2: Wind-Induced Response and Load Estimation / Practical Guide of CFD for Wind Resistant Design.

Kraichnan, R.H., 1970. Diffusion by a random velocity field. The physics of fluids 13, 22-31.

Zhang, Y., Cao, S., Cao, J., 2022. An improved consistent inflow turbulence generator for LES evaluation of wind effects on buildings. Building and Environment 223, 109459.